THE JOURNAL OF BIOLOGICAL CHEMISTRY
Vol. 274, No. 49, Issue of December 3, pp. 35119–35128, 1999
Printed in U.S.A.
© 1999 by The American Society for Biochemistry and Molecular Biology, Inc.

Conformational and Biochemical Differences in the TCR·CD3 Complex of CD8$^+$ *Versus* CD4$^+$ Mature Lymphocytes Revealed in the Absence of CD3γ*

(Received for publication, March 4, 1999, and in revised form, August 27, 1999)

David A. Zapata‡§, Alberto Pacheco-Castro‡¶, Pilar S. Torres‡‖, Almudena R. Ramiro, Ester San José**, Balbino Alarcón**, Laeticia Alibaud‡‡, Bent Rubin‡‡, María L. Toribio**, and José R. Regueiro‡§§**

*From ‡Inmunología, Facultad de Medicina, Universidad Complutense, 28040 Madrid, Spain, the **Centro de Biología Molecular "Severo Ochoa," Consejo Superior de Investigaciones Cientificas, Facultad de Biología, Universidad Autónoma de Madrid, Cantoblanco, 28049 Madrid, Spain, and the ‡‡Centre d'Immunopathologie et de Génétique Humaine, Centre National de la Recherche Scientifique, Centre Hospitalaire Universitaire de Purpan, 31300 Toulouse, France*

Mature CD4$^+$ and CD8$^+$ T lymphocytes are believed to build and express essentially identical surface $\alpha\beta$ T-cell receptor-CD3 (TCR·CD3) complexes. However, TCR·CD3 expression has been shown to be more impaired in CD8$^+$ cells than in CD4$^+$ cells when CD3γ is absent in humans or mice. We have addressed this paradox by performing a detailed phenotypical and biochemical analysis of the TCR·CD3 complex in human CD3γ-deficient CD8$^+$ and CD4$^+$ T cells. The results indicated that the membrane TCR·CD3 complex of CD8$^+$ T lymphocytes was conformationally different from that of CD4$^+$ lymphocytes in the absence of CD3γ. In addition, CD8$^+$, but not CD4$^+$, CD3γ-deficient T lymphocytes were shown to contain abnormally glycosylated TCRβ proteins, together with a smaller, abnormal TCR chain (probably incompletely processed TCRα). These results suggest the existence of hitherto unrecognized biochemical differences between mature CD4$^+$ and CD8$^+$ T lymphocytes in the intracellular control of $\alpha\beta$TCR·CD3 assembly, maturation, or transport that are revealed when CD3γ is absent. Such lineage-specific differences may be important in receptor-coreceptor interactions during antigen recognition.

Mature $\alpha\beta$ T lymphocytes recognize pathogen-derived peptides on antigen-presenting cells by means of the multimeric membrane protein ensemble termed the T-cell receptor (TCR)[1]·CD3 complex. This TCR·CD3 complex includes two clonally distributed variable chains that directly interact with antigens (TCRα and TCRβ) and four invariant polypeptides that regulate assembly and signal transduction (CD3γ, CD3δ, CD3ϵ, and ζ) (1). The assembly of complete TCR·CD3·ζ complexes takes place in a highly ordered manner within the endoplasmic reticulum: first CD3 chains, then TCR chains, and finally ζ chains. Further conformational maturation, including carbohydrate processing, occurs in the Golgi apparatus before exportation of mature complexes to the T cell surface. The biochemical machinery involved in the assembly, processing, and exportation of TCR·CD3 complexes is assumed to be shared by all $\alpha\beta$ T-lineage cells. Thus, CD4$^+$ and CD8$^+$ are believed to build biochemically and conformationally identical antigen receptors, although differences in the numbers that reach or remain at the cell surface have been noted (2). Therefore, the lack of any CD3 chain would be expected to affect to a similar extent the assembly and exportation of TCR·CD3 complexes by mature CD4$^+$ and CD8$^+$ T cells. However, this was not the case in several murine and human CD3 deficiencies (reviewed in Ref. 3). In particular, it has been consistently shown that in the absence of CD3γ or CD3δ, TCR·CD3 expression (or conformation) is more impaired in mature peripheral CD8$^+$ cells than in their CD4$^+$ counterparts, both in human and in murine deficiencies (3–7). Three other observations suggested the existence of CD8$^+$ cell-specific defects in human CD3γ deficiency: first, the proband died after a viral infection (a cytolytic T-cell-dependent function) despite normal antibody responses (helper T-cell-dependent) (8); second, the peripheral blood CD8$^+$ T cell subset was more strongly reduced (5-fold) than the CD4$^+$ T cell subset (only 2-fold) (4); and third, the scanty peripheral CD3γ-deficient CD8$^+$ cells, but not CD4$^+$ cells, failed to grow *in vitro* under optimal stimuli (PHA and allogeneic feeder cells) (4). This paradox may be the reflection either of subset-specific defective maturation of CD3^{low} to CD3^{high} thymocytes in these mutants (3) or of hitherto unrecognized biochemical differences in the assembly or maturation of TCR·CD3 complexes between peripheral CD8$^+$ and CD4$^+$ T lymphocytes, revealed only when certain CD3 chains are absent. Alternatively, as suggested previously (4), the peripheral CD8$^+$ T cells of such CD3 deficiencies may belong to a minor population (in CD3-sufficient individuals) that was relatively expanded when either CD3 chain was absent (9).

The recent availability of *Herpesvirus saimiri* C-488 (HVS)-immortalized mature peripheral CD3γ-deficient CD8$^+$ lymphocytes (5) has allowed us to address this paradox in the case of human CD3γ deficiency, by studying phenotypically and biochemically the TCR·CD3 complex of human CD3γ-deficient CD8$^+$ T cells in comparison with CD4$^+$ T cells lacking CD3γ and with appropriate γ-sufficient controls. The results support the notion that, indeed, there are differences in the way mature

* This work was supported by Ministerio de Educación y Cultura Grant PR112/96, Comunidad Autónoma de Madrid Grant 13/97, Comisión Interministerial de Ciencia y Tecnología Grant SAF96/119, Dirección General de Enseñanza Superior e Investigación Cientifica Grant PM98/91, and Ministerio de Educación y Cultura Grant HF1996/0163 (to J. R. R.). The costs of publication of this article were defrayed in part by the payment of page charges. This article must therefore be hereby marked "*advertisement*" in accordance with 18 U.S.C. Section 1734 solely to indicate this fact.
§ Supported by the Ministerio de Educación y Cultura.
¶ Supported by the Comunidad Autónoma de Madrid.
‖ Supported by the Universidad Complutense de Madrid.
§§ To whom correspondence should be addressed. Tel.: 34-91-3941642; Fax: 34-91-3941641; E-mail: regueiro@med.ucm.es.
[1] The abbreviations used are: HVS, *Herpesvirus saimiri* C-488; MFI, mean fluorescence intensity; TCR, T-cell receptor; PCR, polymerase chain reaction; Endo H, endo-β-*N*-acetylglucosaminidase H; PBL, peripheral blood lymphocyte; mAb, monoclonal antibody; *N*-Gly, *N*-glycosidase F.

This is an Open Access article under the CC BY license.

TABLE I
Antibodies used in this study

Specificity	Name	Type[a]	Dilution	Source (Ref.)
TCRα	αF1	P	100 μg/ml	T-Cell Sciences, Cambridge, MA (13)
TCRα	H36	AS	1:1	O. Acuto, Institut Pasteur, Paris, France (14)
TCRβ	βF1	P	100 μg/ml	Endogene, Woburn, MA
TCR$\alpha\beta$	WT31	P	20 μg/ml	Becton Dickinson, Mountain View, CA
TCR$\alpha\beta$	OKT3a	P	20 μg/ml	Ortho Diagnostic, Raritan, NJ
TCR$\alpha\beta$	BMA031	P	25 μg/ml	Caltag, Burlingame, CA
TCRVβ2–12		P	25 μg/ml	T-Cell Sciences
CD3ε	APA 1/1	AF	1:1000	B. Alarcón, Centro de Biología Molecular Severo Ochoa, Madrid, Spain
CD3ε	2Ad2	AF	1:100	E. L. Reinherz, DANA-FARBER, Boston, MA
CD3ε?	SPV.T3b	S	1:1	J. E. de Vries, The Netherlands Cancer Institute, Amsterdam, The Netherlands
CD3ε?	Cris7	P	20 μg/ml	R. Vilella, Hospital Clinico, Barcelona, Spain
CD3ε	RW2–8C8	AF	1:700	E. L. Reinherz, DANA-FARBER, Boston, MA
CD3ε	X35	P	25 μg/ml	D. Bourel, Centre Régional de Transfusion Sanguine, Rennes, France
CD3δ	APA 1/2	AF	1:1000	B. Rubin, Centre Hospitaliare Universitaire de Purpan, Toulouse, France
CD3ζ	448	AS	1/750	B. Alarcón, Centro de Biología Molecular Severo Ochoa
CD3$\varepsilon\delta$ + $\varepsilon\gamma$	UCHT1	P	25 μg/ml	Immunotech, Marseille, France
CD3$\varepsilon\delta$ + $\varepsilon\gamma$	OKT3	P	50 μg/ml	Ortho Diagnostic
CD3$\varepsilon\delta$ + $\varepsilon\gamma$	F101.01	S	1:10	B. Rubin, CHU de Purpan
CD3$\varepsilon\delta$ + $\varepsilon\gamma$	Leu4	P	50 μg/ml	Becton Dickinson
CD2	T11	P	50 μg/ml	Becton Dickinson
CD4	Leu3a	P	50 μg/ml	Becton Dickinson
CD8	Leu2a	P	50 μg/ml	Becton Dickinson
CD45	anti-HLe-1	P	50 μg/ml	Becton Dickinson
	Isotype controls[b]	P	100 μg/ml	Caltag, Burlingame, CA

[a] P, purified mAb; AF, ascitic fluid mAb; S, mAb supernatant; AS, antiserum.
[b] MOPC-21 (IgG1), UPC-10 (IgG2a), MOPC-195 (IgG2b), and TEPC-183 (IgM).

$CD8^+$ and $CD4^+$ T lymphocytes assemble or process TCR·CD3 complexes, which are revealed when CD3γ is absent.

EXPERIMENTAL PROCEDURES

Immortalization Procedures—-PBLs isolated either from healthy donors or from a CD3γ-deficient (γ^-) individual named D. S. F. were immortalized as described (5, 10, 11). The *Herpesvirus saimiri*-exposed T cells, hereafter referred to simply as HVS cells, had been cultured for 5 years (DSF4, a $CD4^+\gamma^-$ HVS cell line), 4 years (CTO, $CD8^+\gamma^+$, and DSF8, $CD8^+\gamma^-$), 3 years (D8EDTA, $CD8^+\gamma^-$, and AGU, $CD4^+\gamma^+$), or 2 years (RHE, $CD4^+\gamma^+$, and ANZ, $CD8^+\gamma^+$) when the experiments reported here were performed. Cells have always been grown in parallel.

Flow Cytometry Analyses—The expression of different surface markers was studied by flow cytometry according to a standard procedure (12). The antibodies used in these studies are listed in Table I. All commercial antibodies were fluorescein isothiocyanate- or phycoerythrin-conjugated and, for the rest, a second fluorescein isothiocyanate- or phycoerythrin-conjugated antibody (anti-mouse IgG or IgM and anti-rabbit IgG, from Caltag) was used.

Intracellular stainings were done following the protocol described in Ref. 15. In all cases, cell viability was determined by the expression of CD45, and intracellular markers were analyzed within $CD45^+$ cells. Anti-CD1a (OKT6, 1:1000) and anti-CD74 (VICY1, 1:100) ascites were used as negative and positive controls, respectively, for intracellular stainings with ascitic fluids. For intracellular stainings with rabbit antisera, preimmune serum was used as a negative control. Epstein-Barr virus-transformed lymphoblastoid B cells were used as specificity controls.

For comparative stainings the mean fluorescence intensity (MFI) was used, which is defined as the average fluorescence value of the corresponding mAb referred to the logarithmic scale of fluorescence intensity along the x axis of the histograms.

Calcium Flux Measurement—Intracellular Ca^{2+} release was induced in PBLs loaded with the fluorescent dye Fluo3AM (Sigma) according to a standard procedure (12).

Radiolabeling and Immunoprecipitation—For metabolic labeling, at least 10^7 cells were washed once with DPBS (0.14 M NaCl, 8 mM Na_2HPO_4, 1.5 mM KH_2PO_4, 2.7 mM KCl). Then cells were left to become resting by incubation in DPBS supplemented with 1% fetal calf serum for 1 h at 37 °C/5% CO_2. After one more washing with DPBS, cells were resuspended in 300 μl of methionine/cysteine-free RPMI medium (Sigma), supplemented with 5% fetal calf serum, containing 170 μCi of a [^{35}S]Met and [^{35}S]Cys mixture (Amersham Pharmacia Biotech). Cells were then incubated for 30 min at 37 °C/5%CO_2 and afterward an equal amount of "cold" RPMI medium (without [^{35}S]Met and [^{35}S]Cys) was added to the labeling tubes. Cells were incubated in these conditions for 1 h more at 37 °C/5% CO_2. Then cells were washed twice in DPBS and subsequently lysed on ice (45 min incubation) in 1% digitonine-containing lysis buffer (1% digitonine (RBI, Natick, MA), 50 mM Tris-HCl, 150 mM NaCl, 1 mM $MgCl_2$, 0.1 mM EDTA, 1 mM phenylmethylsulfonyl fluoride (Sigma) and 8 mM iodoacetamide (Sigma), pH 7.6). Cell debris was removed by centrifuging the tubes at 2000 × g for 10 min. Then supernatants were collected and centrifuged for 30 min at 14,000 × g to eliminate the smallest cell debris. Again, supernatants, hereafter referred to as lysates, were collected and transferred to new tubes.

The lysates were precleared twice by incubation with Sepharose beads (Amersham Pharmacia Biotech) containing 1% digitonine, followed by a 2-min centrifugation at 12,000 × g in an Eppendorf centrifuge at 4 °C. The precleared supernatants were subsequently incubated for 1.5 h at 4 °C with 0.5 ml of OKT3 or APA1/2 supernatants (anti-CD3$\epsilon\delta/\epsilon\gamma$ or anti-CD3δ, respectively) coupled to protein G-Sepharose beads (Amersham Pharmacia Biotech). The beads were afterward washed five times in lysis buffer. For deglycosylation with endo-β-*N*-acetylglucosaminidase H (Endo H) (Roche Molecular Biochemicals), immunoprecipitates were resuspended, after the last wash, in 45 μl of denaturing buffer (5% SDS, 10% 2-mercaptoethanol) and boiled for 10 min. After a 2-min/12,000 × g centrifugation, supernatants were pipetted to new Eppendorf tubes, dividing each immunoprecipitate in two tubes, one to be deglycosylated (Endo H^+) and the other to be used as non-deglycosylation control (Endo H^-). 4.5 μl of 10× Endo H buffer (0.5 M sodium citrate, pH 5.5) and 1 μl of Endo H (1000 IU/ml) were added to the Endo H^+ samples, which were in turn incubated overnight at 37 °C. The Endo H^- tubes were meanwhile kept at 4 °C. Samples were then resuspended in Laemmli sample buffer and boiled for 5 min before a short spin at 12,000 × g. SDS-polyacrylamide gel electrophoresis was performed on 10% or 12% polyacrylamide gels (see legends to Figs. 5 and 6), and the samples were analyzed by autoradiography or in a PhosphorImager SI (Molecular Dynamics, Sunnyvale, CA). The films were electronically scanned (Bio-Rad Geldoc 2000 analyzer) to determine the relative intensity and molecular weight of each protein.

For surface labeling, at least 10^7 cells were washed twice with phosphate-buffered saline and resuspended in 150 μl of phosphate-buffered saline. Then cells were ^{125}I-labeled using the lactoperoxidase method by adding 2 mCi of $Na^{125}I$ (Amersham Pharmacia Biotech), 30 μl of a 140

IU/ml lactoperoxidase solution (Sigma), and 10-μl aliquots of a 0.06% H_2O_2 solution four times at 5-min intervals. To stop the labeling reaction, a solution of 20 mM KI and 1 mM tyrosine phosphate-buffered saline was added to the tubes (Sigma). The samples were then lysed in a lysis buffer containing 1% Brij 96 (Sigma), 150 mM NaCl, 20 mM Tris-HCl, pH 7.8, 10 mM iodoacetamide, 1 mM phenylmethylsulfonyl fluoride, 1 μg/ml each leupeptin and aprotinin. The lysates were precleared twice with Sepharose beads as described above. Immunoprecipitation was performed with 2–4 μg of APA 1/1 (anti-CD3ε) coupled to protein A-Sepharose beads (Amersham Pharmacia Biotech). This antibody has been shown to coprecipitate CD3γ and CD3δ chains (12), which can be then resolved by deglycosylation. Samples were then divided in two, and after five washings with lysis buffer, one part was digested overnight with *N*-glycosidase F (*N*-Gly$^+$, Roche Molecular Biochemicals), whereas the other was left undigested (*N*-Gly$^-$). Briefly, *N*-Gly$^+$ samples were denatured by boiling for 2 min in 7 μl of a solution containing 0.5% SDS and 0.8% 2-mercaptoethanol. After cooling the samples on ice, 15 μl of *N*-Gly buffer (250 mM Na_2PO_4, pH 8.8, 1% Nonidet P-40, 10 mM EDTA) were added to all tubes, and then 1 μl/sample of 200 unit/ml *N*-Gly was added to the *N*-Gly$^+$ samples. *N*-Gly$^+$ tubes were incubated overnight at 37 °C, whereas *N*-Gly$^-$ tubes were maintained at 4 °C. Finally, all samples, *N*-Gly$^+$ and *N*-Gly$^-$, were resuspended in Laemmli sample buffer, boiled for 5 min before a short spin at 12,000 × *g,* and resolved by SDS-polyacrylamide gel electrophoresis on 12% polyacrylamide gels.

Northern Blot Analysis—Total RNA was isolated with Ultraspec (Biotecx, Houston, TX) following the manufacturer's instructions, and then at least 10 μg of RNA were run on 1% agarose-formaldehyde gels, transferred to nylon membranes, and hybridized as described elsewhere (Ref. 16 and references therein) with ^{32}P-labeled cDNA probes corresponding to the TCR Cα, Cβ (17), Cγ (18), Cδ (19), and pTα. The same blot was subsequently stripped and hybridized with a β-actin probe.

Vβ Usage Analysis by Reverse Transcription-PCR—Total RNA (2 μg) was reverse-transcribed into cDNA using an oligo-dT primer according to the manufacturer's protocol (Roche Molecular Biochemicals). cDNA from HVS-immortalized cells or from PBLs was amplified by PCR using 22 different 5′ Vβ-specific primers (Vβ1-Vβ20; see Fig. 7) together with a common 3′ Cβ-specific primer (20). Amplified products were electrophoresed, transferred to nylon membranes, and analyzed by Southern blot hybridization with a Cβ probe (Jurβ2, 17).

Statistical Analysis—Student's *t* test was used for all comparisons. Only *p* values below 0.05 were considered significant. Data are presented as mean ± S.D.

RESULTS

Peripheral Blood CD8$^+$ Lymphocytes from a Human CD3γ Deficiency Were Functional T Cells with a Normal Vβ Repertoire—The barely detectable surface expression of certain TCR·CD3 epitopes in CD8$^+$ lymphocytes from human CD3γ deficiency (Fig. 1*A* and Ref. 4), together with the fact that they did not grow in optimal T-cell culture conditions (4), could be interpreted as an indication that they were not T lymphocytes at all but rather NK-lineage cells. Our previous phenotypic analysis of such CD8$^+$ lymphocytes did not support that hypothesis for two reasons: 1) most CD8$^+$ cells in CD3γ deficiency were CD8^{bright} (that is, CD8αβ$^+$), whereas CD8$^+$ NK cells are normally CD8^{dull} (CD8αα$^+$); and 2) NK markers (CD16, CD56, and CD57) were not overrepresented within the CD8$^+$ cell subset in CD3γ deficiency (Ref. 4). Nevertheless, an additional phenotypical and functional assay was performed to further ascertain the T-lineage descent of CD3γ-deficient CD8$^+$ cells and to rule out their putative NK-lineage descent. First, Vβ usage within CD8^{bright} cells was assayed by cytofluorometry and found to be normal (Fig. 1*B*). Second, an early TCR·CD3-dependent functional response, namely calcium flux, was tested and found also to be normal (Fig. 2). This ruled out the existence of an early signal transduction defect in CD8$^+$γ$^-$ cells as a cause of the observed selective growth defect. Taken together, these results suggested that peripheral blood CD8$^+$ cells from human CD3γ deficiency were polyclonal, functionally competent T lymphocytes.

The Membrane TCR·CD3 Complex of Immortalized CD3γ-deficient CD8$^+$ T Lymphocytes Was Conformationally Different from That of CD3γ-deficient CD4$^+$ Lymphocytes—The limited number of peripheral blood CD8$^+$ lymphocytes in CD3γ deficiency and our inability to obtain CD8$^+$ T cell lines (4) precluded further studies on the CD8$^+$ T cell subset. This prompted us to try HVS immortalization. An HVS-immortalized γ-deficient T cell line termed DSF8 (CD8αβ$^+$, data not shown) was obtained and characterized phenotypically with a large panel of TCR·CD3-specific mAbs (Fig. 3). For comparative purposes, the results for each mAb are depicted as the MFI ratio of γ$^+$ cells to γ$^-$ cells, either CD8$^+$ (Fig. 3*A, black columns*) or, for comparison, CD4$^+$ (Fig. 3*A, shaded columns*) (5). A γ$^+$:γ$^-$ ratio close to 1 (indicated by the *horizontal dotted line*) reflects an equivalent expression of the epitope detected by that particular mAb in γ$^-$ and γ$^+$ cells (see, for example, CD2 and CD4 or CD8). γ$^+$:γ$^-$ ratios above 1 reflect an impaired expression of the detected epitope by γ$^-$ cells relative to γ$^+$ controls (impaired 2-, 3-, and 4-fold for ratios of 2, 3, and 4, respectively, and so forth). By this criterion, three conclusions emerged. First, all anti-CD3 anti-TCRαβ mAbs used stained both CD4$^+$γ$^-$ and CD8$^+$γ$^-$ cells poorly relative to γ$^+$ controls (γ$^+$:γ$^-$ MFI ratios ≥2; Fig. 3*A*). Second, there were, however, clear

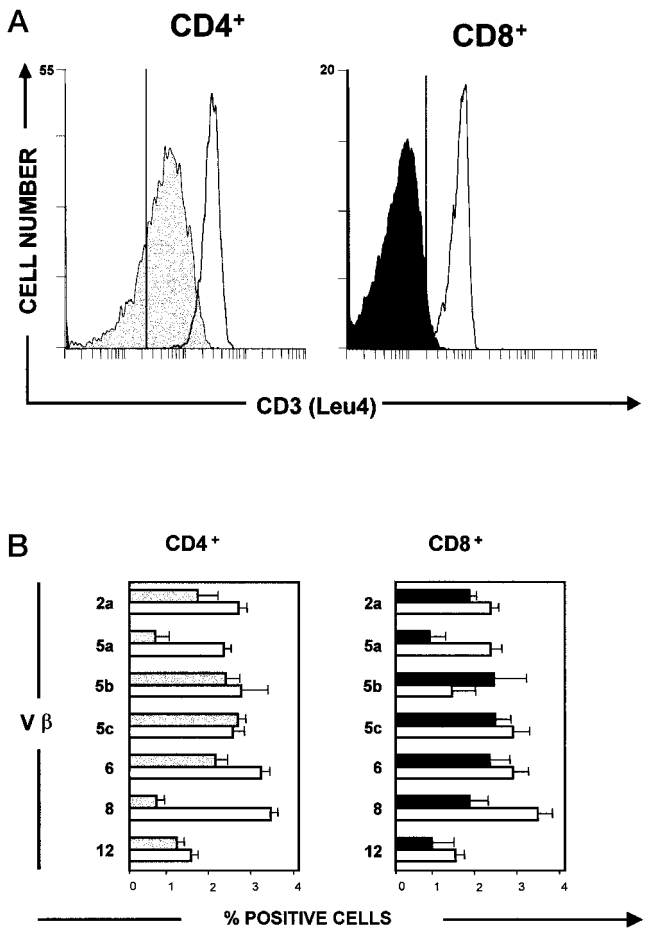

FIG. 1. **Phenotypical analysis of fresh peripheral blood CD3γ-deficient (γ$^-$) T lymphocytes.** *A,* representative reactivity patterns of an anti-CD3ε mAb (Leu4) with γ$^-$ T cells (*filled histograms*) as compared with normal γ$^+$ T cells (*open histograms*), either CD4$^+$ (*left*) or CD8^{bright} (*right*). The profiles are shown as logarithm of relative fluorescence *versus* cell number. The *vertical line* in each panel indicates the upper limit of background fluorescence using an isotype-matched irrelevant mAb. *B,* comparative TCR-Vβ usage by γ$^-$ T cells (*filled bars*) as compared with normal γ$^+$ controls (*open bars*), either CD4$^+$ (*left*) or CD8^{bright} (*right*). Data are given as the mean percentage of positive cells ± S.D. of three different experiments for each indicated Vβ-specific antibody.

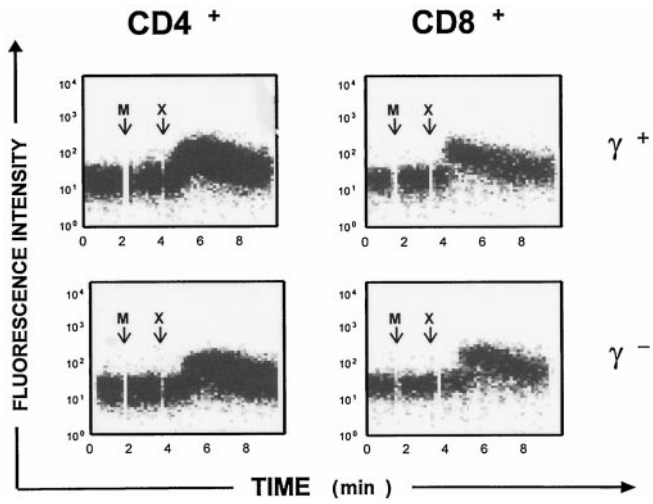

FIG. 2. **Functional analysis of fresh peripheral blood CD3γ-deficient (γ⁻) T lymphocytes.** CD3-mediated calcium mobilization by γ^- T cells (*bottom panels*) as compared with normal γ^+ T cells (*top panels*), either $CD4^+$ (*left*) or $CD8^{bright}$ (*right*). Calcium levels, expressed as relative fluorescence intensity (*y* axis) were measured consecutively: first basally, second after addition of an anti-CD3 mAb (*M*) (IOT3b, 100 μl at 12.5 μg/ml, from Immunotech), and third after cross-linking the mAb (*X*) (human-adsorbed goat anti-mouse IgG (H+L), 40 μl at 1.25 mg/ml, from Caltag). Each manipulation is marked by a *vertical white line* lasting approximately 0.5 min. A representative experiment of two independent assays is shown.

relative staining differences among different mAbs, which were shared by $CD4^+\gamma^-$ and $CD8^+\gamma^-$ cells. Thus, the γ^+:γ^- MFI was around 2 when SPV.T3b was used, but it reached 4 when RW2–8C8, X35, UCHT-1, or OKT3 were analyzed (see Fig. 3*A* and representative stainings of the two patterns in Fig. 3*B*). These results suggest that in addition to displaying lower overall levels of TCR·CD3 complexes, $CD3\gamma^-$ cells were more deficient in the relative expression of certain TCR·CD3 epitopes. The relative expression of other T cell surface molecules was not affected in γ^- cells (*e.g.* CD2, Fig. 3, *A* and *B*). A mAb hierarchy of CD3γ-dependence may be established based on these binding results, as shown in Fig. 3*A*. In general, TCRαβ-specific mAbs bound γ^- T cells more poorly than CD3-specific mAbs, relative to γ^+ controls. It has been shown that TCR·CD3 recognition by certain mAbs may be influenced by glycosylation (*e.g.* WT31, Ref. 21), and we have reported previously that the lack of CD3γ affects TCR·CD3 assembly and glycosylation in $CD4^+$ T cells (12, 22). Therefore, the impaired binding observed in Fig. 3 may in fact be a reflection of the higher or lower glycosylation of the particular epitope recognized by each mAb. Third, as observed in PBLs (Fig. 1*A*), TCR·CD3 binding was significantly more impaired in $CD8^+\gamma^-$ cells than in $CD4^+\gamma^-$ cells, relative to γ^+ controls, with three mAbs: Leu4, 2Ad2, and BMA031 (see representative reactivity patterns in Fig. 3*B*).

These findings showed that, in the absence of CD3γ, immortalized $CD8^+$ cells expressed essentially the same number of membrane TCR·CD3 complexes as $CD4^+$ cells (as shown with SPV.T3b), which were, however, different from those of $CD4^+$ cells (as shown with Leu4, 2Ad2, and BMA031). These results are concordant with PBLs and thus validate the immortalized γ^- cells as a model system to study such differences. The general decrease in TCR·CD3 staining observed in γ^- cells (Fig. 3) could be due to the lack of intracellular subunits (other than CD3γ) to build TCR·CD3 complexes (due, for instance, to degradation), or to poor transport of the γ^- TCR·CD3 complex to the surface. To distinguish between these two possibilities, intracellular stainings of permeabilized γ^- and γ^+ T cells, both $CD4^+$ and $CD8^+$, were performed and compared as above. The results indicated that γ^- cells had slightly more intracellular CD3δ, CD3ε, and TCRβ relative to γ^+ controls (Fig. 4). Therefore, these data are consistent with the hypothesis that the decreased cell surface TCR·CD3 expression seen in γ^- T cells (Fig. 3) is likely due to poor transport of the TCR to the cell surface.

Taken together, the phenotypic data suggested that HVS-immortalized $CD8^+$ cells lacking CD3γ built surface TCR·CD3 complexes, which were conformationally different from those of $CD4^+\gamma^-$ cells, despite the apparent intracellular availability of several relevant TCR and CD3 components other than CD3γ. This was found within the background of a poor transport of γ^- TCR·CD3 complexes to the surface of both cell types. Such $CD8^+$ cell-specific features could be due to: 1) a change in TCR·CD3 subunit composition; 2) a change in TCR·CD3 subunit glycosylation; or 3) a change in accessibility of certain TCR·CD3 epitopes (due to steric hindrance). Further studies were thus undertaken to explore the first two possibilities.

Immortalized CD3γ-deficient CD8⁺, but Not CD4⁺, Lymphocytes Lacked Normal TCRα Chains—Unimmortalized CD3γ-deficient $CD4^+$ cells had previously been analyzed by immunoprecipitation (12, 22) and immunohistochemistry (23) and had been found to contain all TCRαβ and CD3 chains except CD3γ. Thus, the impaired expression of their mutant TCR·CD3 complex could be explained as a simple consequence of the lack of CD3γ on several CD3γ-dependent TCR·CD3 epitopes. The unexpected finding that some of the same epitopes were conformationally different in $CD8^+$ cells prompted us to perform biosynthetic studies on these cells.

First, a [^{35}S]methionine/cysteine pulse-chase immunoprecipitation was done using OKT3 (anti-CD3, Fig. 5*A*) and nonreducing conditions. The results confirmed the lack of CD3γ in $CD8^+\gamma^-$ cells and an impaired association of ζ_2 to the mutant complex, as described previously in unimmortalized $CD4^+\gamma^-$ cells (12, 22). Interestingly, whereas in γ^+ cells, the immature αβ complex (αβi) progressively gave rise to the mature form (αβm), in γ^- cells, the complex had an intermediate size throughout the experiment. Furthermore, the CD3-associated TCRα single chains, either totally (αtg) or partially (αpg) glycosylated, were not detected in γ^- cells. Single TCRβ chains (βtg), in contrast, were present and were apparently more stable in γ^- cells. However, an additional labeled protein running slightly faster than βtg was observed only in γ^- cells. This protein could be a partially glycosylated form of the TCRβ protein, which would be consistent with the hypothesis that the transport and processing of the TCRβ chain is slowed in the absence of CD3γ. Alternatively, the additional labeled protein could represent a new, unidentified protein (see below). Therefore, the TCR heterodimer in $CD8^+\gamma^-$ cells was smaller in size than the normal mature form found in γ^+ cells and lacked the maturation-associated (glycosylation) size changes found in normal TCRαβ heterodimers. In addition, a lack of CD3-associated TCRα chains and CD3ζ was prominent, and an additional protein, probably partially glycosylated TCRβ, was detected in $CD8^+\gamma^-$ cells.

Second, a more detailed analysis of [^{35}S]methionine/cysteine-labeled CD3-associated TCR chains was performed under reducing conditions (Fig. 5*B*), with or without Endo H treatment to remove pre-Golgi *N*-linked oligosaccharides. The results using two different anti-CD3 mAbs (OKT3 and APA1/2) clearly confirmed that the TCR composition of $CD8^+\gamma^-$ cells was different from that of γ^+ controls. Indeed, it involved not only the loss of normal TCRα (αdg) as observed in Fig. 5*A,* but also the addition of another, unidentified 32-kDa protein (Fig. 5*B,* *). By contrast, TCRβ (βdg) was present and normal in size in $CD8^+\gamma^-$ cells. There were also some notable differences be-

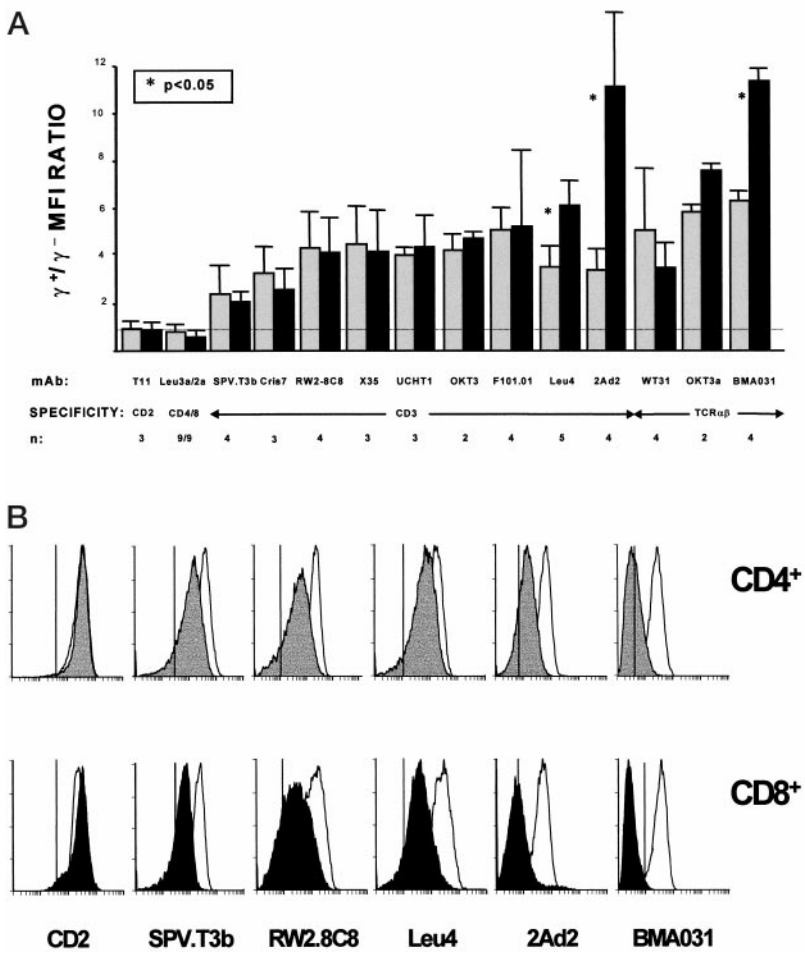

FIG. 3. **Cell surface TCR·CD3 expression in CD8$^+$ as compared with CD4$^+$ HVS-immortalized γ^- T cells.** *A,* comparative expression of several TCR·CD3 epitopes in immortalized γ^- T cells, either CD8$^+$ (*black bars*) or CD4$^+$ (*shaded bars*). Data are given as MFI ratios ± S.D. of γ^+ relative to γ^- cells with the indicated mAbs. MFI ratios above 1 (indicated by the *horizontal dotted line*) reflect an impaired expression of TCR·CD3 on γ^- cells with that particular mAb. The equivalent expression of CD2 and CD4 or CD8 is shown for comparison. *n* indicates the number of independent experiments performed. *B,* representative reactivity patterns of selected anti-TCR·CD3 mAbs with immortalized γ^- T cells (*filled histograms*) as compared with γ^+ controls (*open histograms*), either CD4$^+$ (*top row*) or CD8$^+$ (*bottom row*). The profiles are shown as logarithm of relative fluorescence *versus* cell number. The *vertical line* in each panel indicates the upper limit of background fluorescence using isotope-matched irrelevant mAbs. The reactivity pattern with an anti-CD2 mAb is shown for comparison.

tween γ^- Endo H$^-$ lanes and γ^+ Endo H$^-$ lanes: 1) as shown in Fig. 5*A,* totally glycosylated TCRα (αtg) chains were absent or very reduced in γ^- cells; 2) as in Fig. 5*A,* totally glycosylated TCRβ (βtg) was present in γ^- cells, and an additional labeled protein running slightly faster than βtg (probably partially glycosylated TCRβ) was observed only in γ^- cells; and 3) a very strongly labeled 38-kDa protein was prominent in γ^- cells, coincident in apparent molecular mass with partially glycosylated TCRα (αpg). This protein could represent the glycosylated form of the unidentified 32-kDa protein (Fig. 5*B,* *). However, it may also contain some abnormally glycosylated forms of TCRβ, because the labeling intensity of deglycosylated TCRβ (βdg) apparently exceeds the combined labeling intensity of normal glycosylated TCRβ (βtg) and the additional labeled protein mentioned above. For comparative purposes, immortalized CD4$^+$ cells, both γ^+ and γ^-, and CD8$^+\gamma^-$ cells were [^{35}S]methionine/cysteine-labeled and analyzed under reducing conditions using OKT3, with or without Endo H (Fig. 5*C*). The results indicated that immortalized CD4$^+$ γ^- cells contained normal-sized TCRα (αtg; αpg is not detected in this particular gel) and TCRβ (βtg) proteins and an additional minor labeled protein running slightly faster than βtg (again, probably partially glycosylated TCRβ). CD8$^+\gamma^-$ cells, in contrast, lacked normal TCRα (αtg) but showed normal TCRβ (βtg; partially glycosylated TCRβ is not apparent in this particular gel), and the strongly labeled 38-kDa protein seen in Fig. 5*B,* which perhaps is the glycosylated form of the unknown 32-kDa protein (Fig. 5*C,* *), and some glycosylated form of TCRβ.

Finally, direct immunoprecipitations of TCR chains were carried out in [^{35}S]methionine/cysteine-labeled cells and analyzed under reducing conditions (Fig. 5*D*). The results using an anti-TCRα mAb (αF1, Ref. 13) confirmed the absence of normal TCRα in CD8$^+\gamma^-$ cells but not in CD8$^+\gamma^+$ controls or in CD4$^+$ cells (γ^+ or γ^-). The TCRα chain of the CD8$^+\gamma^+$ sample had slightly smaller (~1 kDa) relative molecular mass than in CD4$^+$ cells, perhaps due to genetic variation (the specific transcripts were also slightly smaller in this particular cell line, see below and Fig. 8). Similar results (*i.e.* lack of normal TCRα in CD8$^+\gamma^-$ cells, sample γ_1^-) were obtained with an unrelated antiserum against TCRα (H36, Ref. 14). The lack of TCRα was confirmed with H36 in an independently derived HVS-immortalized CD8$^+\gamma^-$ cell line termed D8EDTA (sample γ_2^- in Fig. 5*D*). By using an anti-TCRβ mAb (βF1, Ref. 13), totally glycosylated TCRβ (βtg) was detected in CD8$^+\gamma^-$ cells as well in their CD8$^+\gamma^+$ controls, and also in immortalized CD4$^+\gamma^-$ cells and their γ^+ controls (Fig. 5*D*). Interestingly, in addition to βtg, two highly labeled 40- and 42-kDa proteins were observed in CD8$^+\gamma^-$ cells. The proteins were also present in CD8$^+\gamma^+$ controls, although at clearly lower relative levels, despite the fact that the number of cells used for the analysis was similar (5×10^6 in all lanes). Such excess of βF1-reactive proteins in CD8$^+\gamma^-$ cells may explain the significant increase of intracellular βF1 binding observed in CD8$^+\gamma^-$ cells, as compared with CD4$^+\gamma^-$ cells (relative to γ^+ cells, Fig. 4*A*). The two additional proteins are probably glycosylated forms of TCRβ, because they resolved into a single protein with the apparent molecular mass of deglycosylated TCRβ (βdg) after Endo H digestion. Indeed, at least one of these proteins may be present in the very strongly labeled 38-kDa CD3-associated protein observed in CD8$^+\gamma^-$ cells (Fig. 5, *B* and *C*). Alternatively, they may represent unidentified proteins that pair with TCRβ in some T cell types. Similar additional proteins have also been observed in

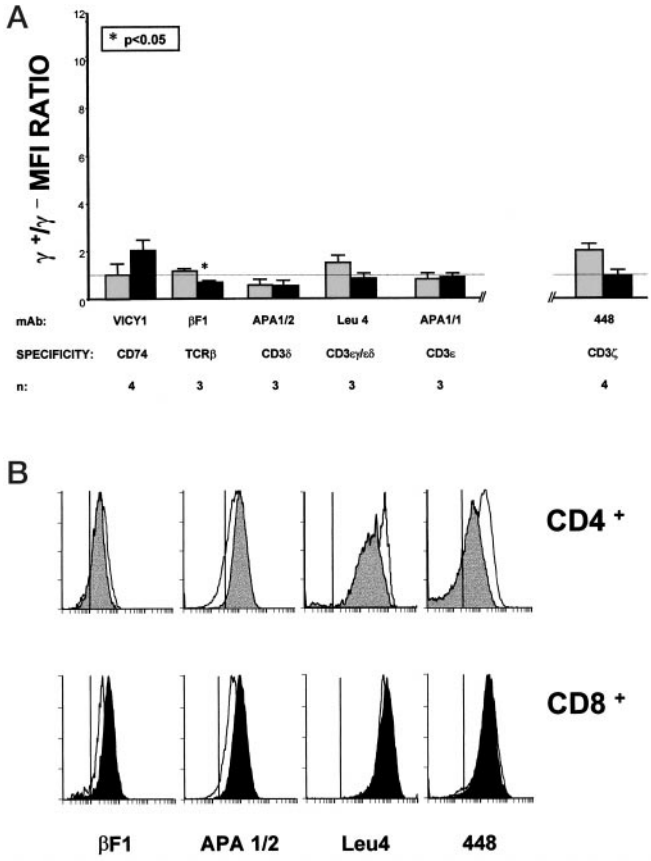

FIG. 4. **Intracellular expression of TCR·CD3 chains in $CD8^+$ as compared with $CD4^+$ HVS-immortalized γ^- T cells after permeabilization.** *A,* comparative intracellular expression of several TCR or CD3 chains in immortalized γ^- T cells, either $CD8^+$ (*black bars*) or $CD4^+$ (*shaded bars*). Data are given as in Fig. 3. MFI ratios above or below 1 (indicated by the *horizontal dotted line*) reflect decreased or increased intracellular levels of the chain detected with that particular antibody, respectively. The expression of CD74 is shown for comparison. *n* indicates the number of independent experiments performed. *B,* representative reactivity patterns of selected anti-TCR and anti-CD3 antibodies with immortalized γ^- T cells (*filled histograms*) as compared with γ^+ controls (*open histograms*), either $CD4^+$ (*top row*) or $CD8^+$ (*bottom row*). The profiles are shown as logarithm of relative fluorescence *versus* cell number. The *vertical line* in each panel indicates the upper limit of background fluorescence using isotype-matched irrelevant mAbs or preimmune serum.

Jurkat cells using βF1 (24).

Collectively, the results of the biosynthetic studies indicated that immortalized $CD8^+$ cells lacking CD3γ contained an abnormally small TCR heterodimer composed of a normal TCRβ chain, some abnormally glycosylated TCRβ chains and an additional unidentified chain that was smaller than normal TCRα and could not be recognized by two unrelated TCRα-specific antibodies. To ascertain whether the intracellular findings were representative of the surface mutant TCR·CD3 complex, $CD8^+\gamma^-$ (and, as a control, $CD8^+\gamma^+$) cells were radioiodinated, lysed, and immunoprecipitated with APA1/1 (anti-CD3ε). Half of the precipitates were digested with *N*-Gly to remove all *N*-linked oligosaccharides before electrophoresis under reducing conditions. The results are shown in Fig. 6*A*. Clear differences were observed between γ^- and γ^+ cells, both in TCR and in CD3 chains. In contrast to biosynthetic results, the amount of CD3-associated TCR proteins was clearly lower (around 3-fold by electronic densitometry) in γ^- cells than in γ^+ cells, so that only major TCR proteins were visible in γ^- samples. With this limitation, the surface-labeled TCR of γ^- cells (Fig. 6*A* *$*) apparently lacked both normal (*i.e.* fully glycosylated) TCRα and TCRβ. The lack of normal TCRα in $CD8^+\gamma^-$ cells confirmed previous biosynthetic results (see above, Fig. 5). The lack of normal TCRβ, in contrast, was not found in those biosynthetic experiments, in which TCRβ was present as a minor but detectable protein (Fig. 5, *B* and *C*). Thus, it cannot be ruled out that the surface TCR of $CD8^+\gamma^-$ cells contained a small amount of fully glycosylated TCRβ that cannot be detected by radioiodination due to the impaired association of surface TCR chains to CD3 in γ^- cells. Two labeled TCR chains, with apparent molecular masses of 40 and 43 kDa, respectively, are discernable in γ^- cells before deglycosylation. Such proteins could in part represent abnormally glycosylated TCRβ, as they are reminiscent in size and intensity of the two highly labeled proteins that coprecipitated with normal TCRβ when βF1 was used (Fig. 5*D*) and, in the case of the smaller one, of the strongly labeled 38-kDa protein coprecipitated with CD3 in Fig. 5, *B* and *C*. The fact that, upon deglycosylation, a major portion of those proteins had the same apparent molecular mass as normal deglycosylated TCRα + TCRβ ((α + β) dg) would lend support to this notion. In addition, a minor portion of the 40- or 43-kDa protein resolved upon deglycosylation into an abnormally small protein of about 30 kDa (Fig. 6*A*, *), which may be identical to the deglycosylated 32-kDa protein precipitated with anti-CD3 in Fig. 5, *B* and *C*. This unidentified protein may represent the protein that is associated with TCRβ in place of normal TCRα in $CD8^+$ γ^-cells. These results confirmed that the surface TCR composition of $CD8^+\gamma^-$ cells was essentially similar to the aberrant intracellular complex characterized previously. However, in the extracellular complex, an impaired association of TCR chains to CD3 components was observed, and neither normal totally glycosylated TCRβ nor TCRα was detectable. Rather, abnormally glycosylated TCRβ and an unidentified 30-kDa chain were observed. $CD8^+\gamma^-$ showed also some clear differences in CD3 chains composition as compared with $CD8^+\gamma^+$ controls, which were not evident in biosynthetic experiments. Indeed, the γ^- sample had, in addition to normal CD3ε, one or more highly labeled proteins with an apparent molecular mass in the range of 25–30 kDa, within the size range of normal CD3γ and CD3δ (Fig. 6*A, ?*). Upon deglycosylation, the protein or proteins had the same apparent molecular mass as normal CD3δ (δdg). Therefore, the 25–30-kDa proteins may be abnormally glycosylated CD3δ. However, due to the increased amount of labeled protein in the deglycosylated γ^- sample, there could also be more than one protein with a size similar to that of CD3δ present. To further substantiate that the highly labeled 25–30-kDa protein(s) of $CD8^+\gamma^-$ cells was abnormally glycosylated CD3δ, it was eluted from the gel, deglycosylated with Endo H, and analyzed by electrophoresis under reducing conditions. Normal CD3γ and CD3δ were analyzed in parallel, as controls. The results are shown in Fig. 6*B*. The normal CD3γ sample showed mature glycosylation, whereas normal CD3δ showed about half mature and half immature glycosylation. The 25–30-kDa protein(s) from γ^- cells did not run at the same size as CD3γ or CD3δ from γ^+ cells, and, in contrast to normal CD3δ, showed no change in size upon Endo H treatment, consistent with mature glycosylation of surface-labeled proteins. Taken together, these results suggested that the surface TCR·CD3 complex of γ^- cells contained normal CD3ε and an additional protein, which most likely represented abnormally glycosylated CD3δ. Experiments are in progress to prove the identity of such protein, by amino acid analysis and partial protease digestion of the deglycosylated form of CD3δ in γ^- *versus* γ^+ cells.

The surface labeling experiments collectively indicated that immortalized $CD8^+\gamma^-$ cells expressed an aberrant TCR·CD3 complex with fewer CD3-associated TCR proteins, lacking nor-

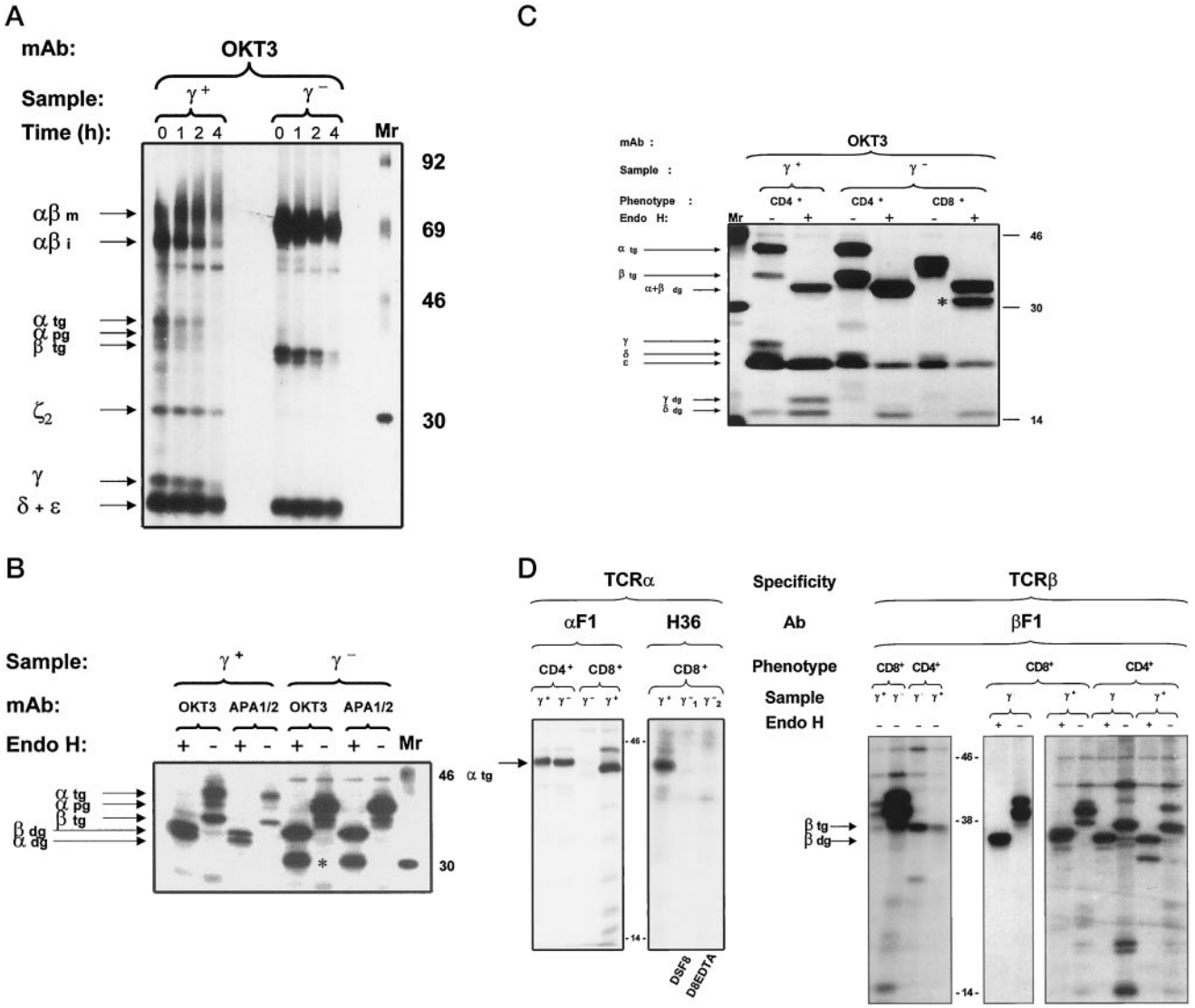

FIG. 5. **Biochemical analyses of CD3γ-deficient TCR·CD3 complexes by metabolic labeling.** *A,* $CD8^+\gamma^-$ cells, and $CD8^+\gamma^+$ cells as a control, were pulsed with [^{35}S]methionine/cysteine for 1.5 h, lysed in a 1% digitonine-containing lysis buffer, and chased for the time periods indicated, before immunoprecipitation with OKT3 (anti-CD3εδ/εγ). Electrophoresis was done under nonreducing conditions (so that TCRαβ dimers were preserved) in a 10% polyacrylamide gel. Positions of the expected proteins are indicated by the *arrows. m,* mature; *i,* immature; *tg,* totally glycosylated; *pg,* partially glycosylated. *B,* cells shown in *A* were labeled, lysed, and precipitated as above with OKT3 or with an anti-CD3δ antibody (APA1/2). Half of each immunoprecipitate was digested with Endo H (+) or left untreated (−) before electrophoresis (12% polyacrylamide) under reducing conditions. Positions of the expected glycosylated (*tg* and *pg*) and deglycosylated (*dg*) proteins are indicated by arrows. The *asterisk* marks the abnormal chain observed in γ^- cells after Endo H treatment. *C,* $CD4^+\gamma^-$ cells, $CD4^+\gamma^+$ cells as controls, and $CD8^+\gamma^-$ cells for comparison were labeled with [^{35}S]methionine/cysteine, lysed, precipitated with OKT3, and digested, where indicated, before electrophoresis (12% polyacrylamide) under reducing conditions. *D, left,* $CD8^+\gamma^-$ cells were labeled with [^{35}S]methionine/cysteine, lysed, precipitated with the indicated TCRα-specific antibodies, and electrophoresed (12% polyacrylamide) under reducing conditions. $CD8^+\gamma^+$, $CD4^+\gamma^-$, and $CD4^+\gamma^+$ cells were included for comparison. For immunoprecipitations with H36, an independently derived HVS-immortalized $CD8^+$ γ^-cell line termed D8EDTA (sample γ^-_2) was analyzed in parallel with DSF8 (normally termed γ^-, but in this particular immunoprecipitation termed γ^-_1). *Right,* $CD8^+$ and $CD4^+$ cells (γ^- and γ^+) were [^{35}S]methionine/cysteine-labeled, lysed, immunoprecipitated with the TCRβ-specific antibody βF1, and digested with Endo H (where indicated) before electrophoresis under reducing conditions in a 12% polyacrylamide gel.

mal TCRα and normally glycosylated TCRβ among them, and with what appeared to be abnormally glycosylated forms of TCRβ and CD3δ, together with an unidentified 30-kDa protein (in deglycosylated form), which may represent the protein paired with TCRβ on the γ^- cell surface. Some of these biochemical results were reminiscent of $TCR\gamma\delta^+$ cells (25), but the possibility that $CD8^+\gamma^-$ cells were $TCR\gamma\delta^+$, rather than aberrant $TCR\alpha\beta^+$, was ruled out by staining with γδ-specific monoclonals TCRδ1 (26) and 11F2 (27) (data not shown) and by Northern blot analysis (see below).

The aberrant TCR of $CD8^+\gamma^-$ cells was not present in $CD4^+\gamma^-$ cells or in γ^+ controls ($CD4^+$ or $CD8^+$). Therefore, it could explain the selective conformational differences detected in peripheral blood (4, 7) or immortalized (Ref. 5 and the present study) $CD8^+\gamma^-$ cells by cytofluorometry. However, it was necessary to rule out the possibility that $CD8^+\gamma^-$ cells were an aberrant clone. To this end, first, Vβ usage was tested by reverse transcription-PCR and found to be comparable to matched controls (32% of the 22 Vβ genes tested; normal range, 31–45%; Fig. 7, γ^-_1 HVS). Second, the lack of TCRα was confirmed on an independently derived HVS-immortalized $CD8^+\gamma^-$ T-cell line termed D8EDTA (Fig. 5*D*, *Sample* γ^-_2 HVS). This T-cell line was also oligoclonal (33% of the Vβ genes tested, Fig. 7, γ^-_2 HVS), but with a different repertoire than γ^-_1 HVS. These patterns were compatible with the variable predominance of Vβ gene usage in HVS-immortalized peripheral T

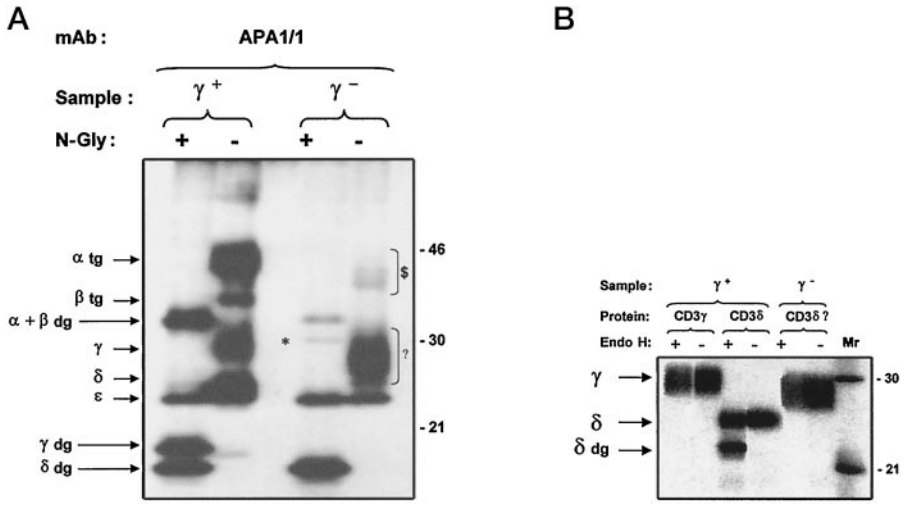

FIG. 6. **TCR·CD3 immunoprecipitation of radioiodinated CD8$^+$ γ$^-$ cells and CD8$^+$ γ$^+$ cells as controls.** *A,* CD8$^+$ cells, either γ$^+$ (*left*) or γ$^-$ (*right*), were surface-labeled with ^{125}I, lysed in a 1% Brij96-containing buffer, precipitated with an anti-CD3ε mAb (APA1/1) and digested, where indicated (+), with *N*-Gly before electrophoresis under reducing conditions in a 12% polyacrylamide gel. *B,* certain CD3 proteins were eluted from the experiment shown in *A* and digested with Endo H, where indicated (+), before electrophoresis under reducing conditions in a 12% polyacrylamide gel. The positions of the expected glycosylated (*tg*) or deglycosylated (*dg*) proteins are indicated by *arrows*. $ and ? mark the abnormal glycosylated CD3-associated TCR and CD3δ chains of CD8$^+$ γ$^-$ cells, respectively. *marks the putative abnormal deglycosylated TCRα chain of CD8$^+$ γ$^-$ cells.

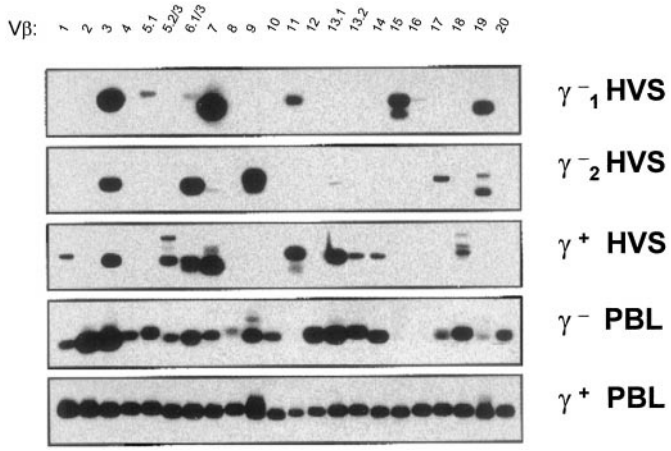

FIG. 7. **TCR Vβ usage by HVS-immortalized CD8$^+$ γ$^-$ cells.** 22 Vβ-specific reverse transcription-PCR were performed as described under "Experimental Procedures," and reverse transcription-PCR products were subsequently hybridized with a ^{32}P-labeled constant TCRβ probe. Two independently derived CD8$^+$γ$^-$ T cell lines (γ$^-_1$ or DSF8 and γ$^-_2$ or D8EDTA (see the legend to Fig. 5*D*)) were compared with normal CD8$^+$γ$^+$ T cells (γ$^+$ *HVS*). Fresh peripheral blood T cells, both γ$^-$ (γ$^-$ *PBL*) and γ$^+$ (γ$^+$ *PBL*) were analyzed in parallel and are included for comparison. The numbers indicate the particular Vβ amplified in each lane.

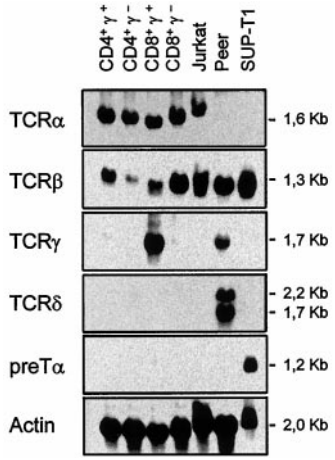

FIG. 8. **Analysis of TCRα, TCRβ, TCRγ, TCRδ, and pTα gene transcription in immortalized CD4$^+$ γ$^+$ and γ$^-$ or in CD8$^+$ γ$^+$ and γ$^-$ cell lines.** Northern blots of total RNA isolated from the indicated cell sources were hybridized with specific ^{32}P-labeled probes, as depicted. Wild type Jurkat cells (TCRαβ$^+$), Peer (TCRγδ$^+$), or SUP-T1 (immature pTα-expressing lymphocytes (16)) were analyzed in parallel. In all cases, β-actin mRNA expression served as an internal positive control.

cells previously described (28).

TCR Gene Expression Was Normal in Immortalized CD3γ-deficient CD8$^+$ Lymphocytes—The lack of normal TCRα in CD8$^+$γ$^-$ cells suggested the possibility that they expressed alternative mature (γδ$^+$) or immature (βpTα$^+$) TCR ensembles. To explore such possibilities, total RNA was isolated from CD8$^+$γ$^-$ cells, and from appropriate controls, and probed for several TCR specific transcripts by Northern analyses (Fig. 8). The results demonstrated that CD8$^+$γ$^-$ cells contained normal levels and sizes of mature TCRα and TCRβ mRNA, whereas they lacked expression of TCRδ, TCRγ, and pTα transcripts. In addition, they did not display germline transcription at the TCR locus and, therefore, T early α transcripts were absent (data not shown). These results support the conclusion that CD8$^+$γ$^-$ cells are not NK cells, nor γδ T cells. Interestingly, they express the TCRα gene at the transcriptional level, although it is apparently not expressed at the protein level.

DISCUSSION

In the present study, we have investigated TCR·CD3 assembly and expression in immortalized natural mutant CD8$^+$ and CD4$^+$ T lymphocytes lacking CD3γ. We were prompted to undertake this study by the unexpected observation that peripheral blood TCR·CD3 expression was more impaired in CD8$^+$ than in CD4$^+$ cells when CD3γ is absent (Refs. 4 and 5 and Fig. 1*A*). Despite their phenotypical defect, CD8$^+$γ$^-$ cells were functional (Fig. 2). Therefore, we tried to understand the mechanisms behind the feeble expression of surface TCR·CD3 on those cells. The unexpected finding was that, in addition to lacking CD3γ, immortalized CD8$^+$γ$^-$ cells, but not CD4$^+$γ$^-$ cells, lacked or expressed few mature TCRα chains (see below).

The consequence of this biochemical finding was that membrane TCR·CD3 complexes from immortalized CD3γ-deficient CD8$^+$ T cells were conformationally different from those of CD3γ-deficient CD4$^+$ T cells or normal CD8$^+$ and CD4$^+$ T cells (Fig. 3). These conformational differences may explain the selective TCR·CD3 expression impairment detected previously in peripheral blood (4, 7)[2] or immortalized (Ref. 5 and present data) murine or human CD8$^+$γ$^-$ T cells by cytofluorometry. Greater sensitivity of CD8$^+$ cells than CD4$^+$ cells to the absence of CD3γ (in terms of TCR·CD3 surface expression) might be related to differences in the intracellular control of αβ TCR assembly, maturation, and/or transport between the two lin-

[2] M. van Tol, personal communication.

eages. The lower levels of surface αβ TCR found in normal mature $CD8^+$ T lymphocytes (2) may be the reflection of such biochemical differences (thus qualitative rather than quantitative) and perhaps relevant in the context of receptor-coreceptor interactions (see below). Indeed, the comparative staining of peripheral blood $CD4^+$ and $CD8^+$ cells using a broad panel of TCR·CD3-specific mAbs revealed that, in contrast to expectations, certain mAbs stained $CD8^+$ cells better than $CD4^+$ cells.[3] A similar situation, *i.e.* increased sensitivity of $CD8^+$ *versus* $CD4^+$ cells in TCR·CD3 expression, has also been observed in mice lacking CD3δ (3, 6). The biochemical basis, however, remained unexplored, perhaps due to the scant peripheral blood lymphoid compartment.

A further study of the influence of CD3γ deficiency on expression of other TCR·CD3 components was performed. Pulse-chase experiments clearly showed the following points: 1) absence of CD3γ chains, 2) absence of CD3ζ chain coprecipitation, and 3) absence of TCRαβ heterodimer maturation in $CD8^+\gamma^-$ T cells (Fig. 5*A*). In addition, TCRβ chains seemed more stable, a finding that, together with absence of CD3ζ coprecipitation and of TCRαβ heterodimer maturation, strongly indicated that TCR·CD3 complexes (or at least most of them) stayed in the endoplasmic reticulum (29). The same results were obtained when several different anti-TCR·CD3 mAbs were used in the other immunoprecipitations.

Nonglycosylated TCRα chains have a molecular mass of about 30 kDa, and partially or fully glycosylated TCRα chains have molecular masses of about 40–45 kDa (up to six *N*-linked sugars). Nonglycosylated TCRβ chains have a molecular mass of 35 kDa, and partially or fully glycosylated TCRβ chains have a molecular mass of about 37–40 kDa. Deglycosylation experiments with Endo H demonstrated that deglycosylated TCRβ chains from the CD3γ-deficient $CD4^+$ or $CD8^+$ cells migrate to the same position. However, deglycosylated TCRα chains from CD3γ-deficient $CD8^+$ T cells have a molecular mass of 2–3 kDa lower than normal (32–34 *versus* 30–32 kDa; see Fig. 5, *B* and *C*). As TCR Cα cDNA sequences in $CD4^+$ and $CD8^+$ CD3γ-deficient T cells are the same as in normal T cells,[4] the most logical explanation seems to be that TCRα chains from CD3γ-deficient $CD8^+$ T cells are more easily deglycosylated compared with CD3γ-deficient $CD4^+$ T cells (or normal T cells). This may be due to the fact that TCRα chains in CD3γ-deficient $CD8^+$ T cells are more immature than those of CD3γ-deficient $CD4^+$ T cells or normal T cells. It is likely that immature TCRα loses recognition by αF1 and other Cα-specific reagents. Indeed, the αF1 monoclonal recognizes an exposed epitope spanning residues 141–159 of the Cα domain (13), including an Asn residue, which is one of the four potential *N*-glycosylation sites of the human Cα domain (30). Loss of recognition by αF1 has been reported previously in a Jurkat variant lacking the transmembrane and cytoplasmic domains of TCRα (31). Parallel studies on CD3γ-deficient Jurkat T cells have shown that 1) an inverse relationship exists between the amount of TCRα chains coprecipitated and the amounts of CD3γ chains produced in a T cell line, and 2) the production of only partially glycosylated CD3γ chains influences TCRα chain glycosylation.[5]

Abnormal assembly and glycosylation of the TCR·CD3 complex have been reported previously in $CD4^+\gamma^-$ cells (12, 22). However, the differences in TCRα observed in $CD8^+$ *versus* $CD4^+$ γ-deficient cells have not been reported previously. Nascent TCRα chains have been shown to be uniquely unstable in immature murine T cells (32), perhaps because of altered processing of oligosaccharide side-chains in the endoplasmic reticulum (33). These differences are believed to cause the reduced TCR·CD3 expression observed in immature *versus* mature T lymphocytes (34) or in transfected eukaryotic cells (35). Similarly, our results suggest that human mature $CD8^+$ and $CD4^+$ T lymphocytes may differ in the intracellular control of TCR·CD3 assembly, maturation, or transport. Such differences would be revealed when CD3γ is absent, particularly in TCRα, which is the most unstable chain.

The most difficult data to interpret are those from external labeling of TCR·CD3 complexes from CD3γ-deficient $CD8^+$ T cells: 1) few TCR molecules are labeled/coprecipitated (in proportion to CD3 chains precipitated), and 2) deglycosylated TCRα chains have an apparent molecular mass lower than deglycosylated TCRα chains from normal T cells (Fig. 6). In addition, CD3γ-deficient $CD8^+$ T cells seem to express CD3δ (and probably TCRβ) chains, which are more glycosylated than the normal counterparts. Thus, are the TCR·CD3 complexes on the surface of CD3γ-deficient $CD8^+$ T cells normal, with expression of low levels of mature TCRα chains? Or alternatively, are the TCR·CD3 complexes on the surface of CD3γ-deficient $CD8^+$ T cells constructed with a TCRα chain different from normal TCRα chains?

Despite the observed biochemical differences in the TCR·CD3 complex of $CD8^+\gamma^-$ *versus* $CD4^+\gamma^-$ cells, their functional behavior was undistinguishable when several CD3-induced activation events were analyzed (5). Thus, it may well be that the peripheral T lymphocytes that we can analyze when CD3γ is absent are those carrying TCR·CD3 complexes that are conformationally compatible with the corresponding coreceptor. A direct interaction of the TCR with CD4 and CD8 has been proposed before (36–39).

TCR·CD3-induced calcium flux was normal in $CD4^+$ and $CD8^+$ CD3-deficient PBLs (Fig. 2) and HVS-immortalized (5) T cells. However, it was partially impaired in an unimmortalized $CD4^+$ T cell line (DIL2) derived from the same donor (12). This discrepancy may have been due to clonal variation of DIL2 or, alternatively, to differences in the selective pressures imposed by the culture conditions. DIL2 was grown with PHA, which is a strong TCR·CD3 stimulant, whereas HVS cells grow by TCR·CD3-independent interactions (11) and may therefore be more representative of PBL behavior.

Acknowledgments—We thank Drs. A. Arnáiz-Villena and A. Corell for sharing DSF4 cells, Drs. C. Trigueros and A. Alvarez for technical support, and Drs. O. Acuto, J. Borst, M. Brenner, D. Jaraquemada, E. L. Reinherz, and J. E. de Vries for mAb samples. Hoffmann-LaRoche is gratefully acknowledged for the continuous supply of recombinant IL-2.

REFERENCES

1. Wang, B., Simpson, S. J., Höllander, G. A., and Terhorst, C. (1997) *Immunol. Rev.* **157,** 53–60
2. Thibault, G., and Bardos, P. (1995) *J. Immunol.* **154,** 3814–3820
3. Kappes, D., Alarcón, B., and Regueiro, J. R. (1995) *Curr. Opin. Immunol.* **7,** 441–447
4. Timón, M., Arnaiz-Villena, A., Rodríguez-Gallego, C., Pérez-Aciego, P., Pacheco, A., and Regueiro, J. R. (1993) *Eur. J. Immunol.* **23,** 1440–1444
5. Pacheco-Castro, A., Alvarez-Zapata, D., Serrano-Torres, P., and Regueiro, J. R.. (1998) *J. Immunol.* **161,** 3152–3160
6. Dave, V. P., Cao, Z., Browne, C., Alarcón, B., Fernández-Miguel, G., Lafaille, J., de la Hera, A., Tonegawa, S., and Kappes, D. J. (1997) *EMBO J.* **16,** 1360–1370
7. Haks, M. C., Krimpenfort, P., Borst, J., and Kruisbeek, A. M. (1998) *EMBO J.* **17,** 1871–1882
8. Arnaiz-Villena, A., Timón, M., Corell, A., Pérez-Aciego, P., Martín-Villa, J. M., and Regueiro, J. R.. (1992) *N. Engl. J. Med.* **327,** 529–533
9. Leo, O., Foo, M., Forman, J., Shivakumar, S., Rabinowitz, R., and Bluestone, J. A. (1988) *J. Immunol.* **141,** 37–44
10. Biesinger, B., Müller-Fleckenstein, I., Simmer, B., Lang, G., Wittman, S., Platzer, E., Desrosiers, R. C., and Fleckenstein, B. (1992) *Proc. Natl. Acad. Sci. U. S. A.* **89,** 3116–3119
11. Meinl, E., Hohfeld, R., Wekerle, H., and Fleckenstein, B. (1995) *Immunol. Today* **16,** 55–58
12. Pérez-Aciego, P., Alarcón, B., Arnaiz-Villena, A., Terhorst, C., Timón, M., Segurado, O. G., and Regueiro, J. R.. (1991) *J. Exp. Med.* **174,** 319–326

[3] P. S. Torres, unpublished data.
[4] D. A. Zapata, unpublished data.
[5] A. Huchenq, L. Alibaud, C. Bouchouata, C. Gouaillard, R. Llobera, A. Alcover, J. Arnaud, and B. Rubin, submitted for publication.

13. Henry, L., Tian, W. T., Rittershaus, C., Ko, J. L., Marsh, H. C. Jr., and Ip, S. H. (1989) *Hybridoma* **8,** 577–588
14. Fabbi, M., Acuto, O., Bensussan, A., Poole, C. B., and Reinherz, E. L. (1985) *Eur. J. Immunol.* **15,** 821–827
15. Dodi, A. I., Brett, S., Nordeng, T., Sidhu, S., Batchelor, R. J., Lombardi, G., Bakke, O., and Lechler, R. I. (1994) *Eur. J. Immunol.* **24,** 1632–1639
16. Ramiro, A. R., Trigueros, C., Márquez, C., San Millán, J. L., and Toribio, M. L. (1996) *J. Exp. Med.* **184,** 519–530
17. Yoshikai, Y., Antoniou, D., Clark, S. P., Yanagi, Y., Sangster, R., van den Elsen, P., Terhorst, C., Mak, T. W. (1984) *Nature* **312,** 521–524
18. Yoshikai, Y., Toyonaga, B., Koga, Y., Kimura, N., Greisser, I. I., and Mak, T. (1987) *Eur. J. Immunol.* **17,** 119–126
19. Borst, J., Wicherink, A., Van Dongen, J. J., De Vries, E., Comans-Bitter, W. M., Wassenaar, F., and Van den Elsen, P. (1989) *Eur. J. Immunol.* **19,** 1559–1568
20. Choi, Y., Kotzin, B., Herrron, L., Callahan, J., Marrack, P., and Kappler, J. (1989) *Proc. Natl. Acad. Sci. U. S. A.* **86,** 8941–8945
21. van de Griend, R. J., Borst, J., Tax, W. J. M., and Bolhuis, R. L. (1988) *J. Immunol.* **140,** 1107–1110
22. Alarcón, B., Regueiro, J. R., Arnaiz-Villena, A., and Terhorst, C. (1988) *N. Engl. J. Med.* **319,** 1203–1208
23. Arnaiz-Villena, A., Pérez-Aciego, P., Ballestín, C., Sotelo, T., Pérez-Seoane, C., Martín-Villa, J. M., and Regueiro, J. R.. (1991) *Lab. Invest.* **64,** 675–681
24. San José, E., Sahuquillo, A. G., Bragado, R., and Alarcón, B. (1998) *Eur. J. Immunol.* **28,** 12–21
25. Krangel, M., Bierer, B., Devlin, P., Clabby, M., Strominger, J., McLean, J., and Brenner, M. (1987) *Proc. Natl. Acad. Sci. U. S. A.* **84,** 3817–3821
26. Band, H., Hochstenbach, F., McLean, J., Hata, S., Krangel, M. S., and Brenner, M. (1987) *Science* **238,** 682–684
27. Borst, J., van Dongen, J. J., Bolhuis, R. L., Peters, P. J., Hafler, D. A., de Vries, E., and van de Griend, R. J. (1988) *J. Exp. Med.* **167,** 1625–1644
28. Fickenscher, H., and Fleckenstein, B. (1994) in *Methods in Molecular Genetics* (Adolph A., ed) Vol. 4, p. 345–362, Academic Press, San Diego
29. Arnaud, J., Huchenq, A., Vernhes, M. C., Caspar-Bauguil, S., Lenfant, F., Sancho, J., Terhorst, C., and Rubin, B. (1997) *Int. Immunol.* **9,** 615–626
30. Yanagi, Y., Chan, A., Chin, B., Minden, M., and Mak, T. W. (1985) *Proc. Natl. Acad. Sci. U. S. A.* **82,** 3430–3434
31. Arnaud, J., Cayrou, C., Llobera, R., and Rubin, B. (1997) *Immunogenetics* **45,** 311–319
32. Kearse, K., Roberts, J. L., Munitz, T., Wiest, D. L., Nakayama, T., and Singer, A. (1994) *EMBO J.* **13,** 4504–4514
33. Kearse, K., Williams, D., and Singer, A. (1994) *EMBO J.* **13,** 3678–3686
34. Kearse, K., Takahama, Y., Punt, J. A., Sharrow, S. O., and Singer, A. (1995) *J. Exp. Med.* **181,** 193–202
35. Chung, S., Wucherpfenning, K. W., Friedman, S. M., Hafler, D. A., and Strominger, J. L. (1994) *Proc. Natl. Acad. Sci. U. S. A.* **91,** 12654–12658
36. Vignali, D. A., Carson, R. T., Chang, B., Mittler, R. S., and Strominger, J. L. (1996) *J. Exp. Med.* **183,** 2097–2107
37. Rojo, J. M., Saizawa, K., and Janeway, C. A., Jr. (1989) *Proc. Natl. Acad. Sci. U. S. A.* **86,** 3311–3315
38. Hoo, W. S., and Kranz, D. M. (1993) *J. Immunol.* **150,** 4331–4337
39. Garcia, K. C., Scott, C. A., Brunmark, A., Carbone, F. R., Peterson, P. A., Wilson, I. A., and Teyton, L. (1996) *Nature* **384,** 577–581